

Implementation of Unmanned Aerial Vehicles in the Automated Assessment of Geodetic Database Validity

Klaudia Maciąg^{1*}, Michał Maciąg¹, Przemysław Leń²

¹ Faculty of Environmental Engineering and Geodesy, University of Life Sciences in Lublin, ul. Akademicka 13, 20-950 Lublin, Poland

² Faculty of Geodesy and Geotechnics, Rzeszów University of Technology, al. Powstańców Warszawy 12, 35-959 Rzeszów, Poland

* Corresponding author's e-mail: klaudia.maciag@up.lublin.pl

ABSTRACT

Nowadays, the progress of technology covers, among other things, the development of modern techniques and high technologies used in land surveys. Unmanned aerial vehicles (UAVs), as a good alternative to conventional land survey techniques, have currently played an increasing role. The advantages of using unmanned aerial vehicles in photogrammetric measurements include a relatively short mission time for large-area surveys. In addition, photogrammetric products have a wider range of applications compared with conventional geodetic surveys. Many scientific publications delve into the quality of photogrammetric products, but the accuracy of UAVs in the context of geodetic standards has not been investigated in full. In this paper, the authors attempt to fill the observed research gap. The research has analysed the position of objects recorded in geodetic databases referring to their counterparts based on an accurate “true” orthophotomap from a photogrammetry campaign employing an unmanned aerial vehicle. The outcomes were referenced with land survey accuracy standards set out by relevant legislation. To ensure a smooth assessment of the result's accuracy a computing algorithm with a module for selecting comparable points and verifying the results was designed. The tool can be implemented in surveys carried out in any area thanks to open-source GIS software. The analysis showed that a detailed orthophotomap delivered using UAVs can be a valuable data source on objects recorded in geodetic databases covering selected cadastral and topographic objects and land development components. A general verification of the accuracy and validity of a geodetic numerical map and preliminary detection of areas for potential updates can be a particularly useful application of photogrammetry.

Keywords: UAV, orthophotomap, base map, algorithm, accuracy.

INTRODUCTION

The dynamic increase in the technology advancement level of unmanned aerial vehicles (UAVs) and an increasingly broad range of their application have raised interest in implementing drones in land survey tasks. The use of UAVs in surveys has been a current topic of numerous scientific papers in many countries of Europe, including Poland [1,2], Slovakia [3], Romania [4], Germany [5–7], Croatia [8], Italy [9], Switzerland [10], Greece [11], the Netherlands [12–15], Denmark [16], Spain [17–21], and in Asian countries including China [22–26], India [27], Indonesia

[28], and North America [29–31], and in Africa: Namibia [32], and Ethiopia [33]. Surveys were also conducted in Australia [34–36]. Many researchers describe the possible uses of drones in areas such as real estate cadastre [37–40], land consolidation [41], photogrammetry and remote sensing [42], and surveying [43, 44]. A huge advantage of UAVs used in land surveying for high-speed photogrammetric flights maintaining accurate and detailed land information. Therefore, surveying with UAVs is much more viable than using the time-consuming and less efficient conventional surveying methods. For large-area surveys, using UAVs can be a key condition for

conducting the planned work such as creating 3D models of open-cast mines [45], remote sensing of vegetation in urban areas [46], kinematic analysis of maritime cliffs [47] and supporting the processes of Building Information Modeling (BIM) [48–53].

The real estate cadastre is another potential area to employ unmanned aerial vehicles. Kurczyński et al. write about studies concerning the possibility of acquiring data on the geometry of buildings based on the orthophotomap, slope maps and 3D terrain models generated based on photogrammetric images retrieved using the UAV technology [54]. Their studies compared the coordinates retrieved from 3D models against data derived from direct field surveys involving GNSS techniques and a tacheometry. The analyses indicate that UAV surveys can be used in acquiring data on the geometry of buildings. Data acquired using UAV technology are comparable with the results of GNSS surveys and conventional surveys. The analysis presented by the authors revealed a necessity for regular updates of data acquired by UAVs and verifying these data against field survey results. Also mentioned was the impossibility of conducting photogrammetry surveys for objects shadowed or covered by other objects [55].

In addition, Puniach et al. examined the options of using UAVs to update the real estate cadastre data for areas affected by landslides. Their articles concluded that data acquired from UAVs can be used in updating the real estate cadastre and the factor affecting the accuracy of photogrammetric products is the number of checkpoints used [56].

Crommelinck et al. presented the possibility of using an orthophotomap for acquiring data on cadastral boundaries using computer vision. The authors highlighted that the existing procedures usually require a considerable amount of time spent on fieldwork and that many processes are manual. They describe how the mapping process can be improved using automated detection of the objects' geometry. According to surveys, object contours are detected with an accuracy of 80%. The authors emphasised that the approach they had presented could considerably accelerate the process of delineating cadastral boundaries and updating maps [57, 58].

In their studies, Šafař et al. delve into options of using UAV photogrammetry and laser scanning to acquire cadastral data in the Czech Republic.

Their research showed that both the point cloud and the orthophotomap achieved the assumed accuracy. Among the advantages of the possibility to update cadastral maps using UAV technology, the authors mentioned improved negotiations with real estate owners, direct comparisons of data sets with archival data, oblique views, the effective production of digital maps, and independent verification of objects. In turn, the drawbacks of this solution include the necessity to perform additional surveys using conventional methods, expensive equipment and software, and the necessity to provide training to personnel and consider local conditions in mission planning [59].

Pyka et al. in their studies give an overview of good practices and recommendations for planning and processing UAV images. Thus, they also highlight the absence of publications dedicated to the accuracy of UAV products within the meaning of land surveying in the world reference literature [60]. This paper is an attempt to fill the indicated research gap.

An area in which UAVs can be used is preparation for land consolidation. Photogrammetric flights using UAVs facilitate the efficient generation of a current large-area orthophotomap, which can be a basic material used in the entire land consolidation process. The orthophotomaps can be used, among other things, for preparing land consolidation projects and identifying differences between data acquired from a geodetic and cartographic records centre and the current field status. They can also provide auxiliary materials for communication between land consolidation contractors and participants.

The object of the research described in this article is a detailed assessment of the possible uses of a UAV-based orthophotomap in updating the geodetic spatial database resources. The research involved objects retrieved from a geodetic and cartographic records centre and dedicated high-accuracy orthophotos acquired from unmanned aerial vehicles. During the work, an automated algorithm for selecting and comparing input data and analysing data accuracy was designed.

The tool was implemented in the analysis of potential uses of a digital orthophotomap for updating and supplementing geodetic databases such as EGİB (land and buildings register), BDOT500 (topographic objects database) and GESUT (utilities network database) for the village of Turze Pole, in the district of Brzozów, south-eastern Poland. Figure 1 shows the study area location.

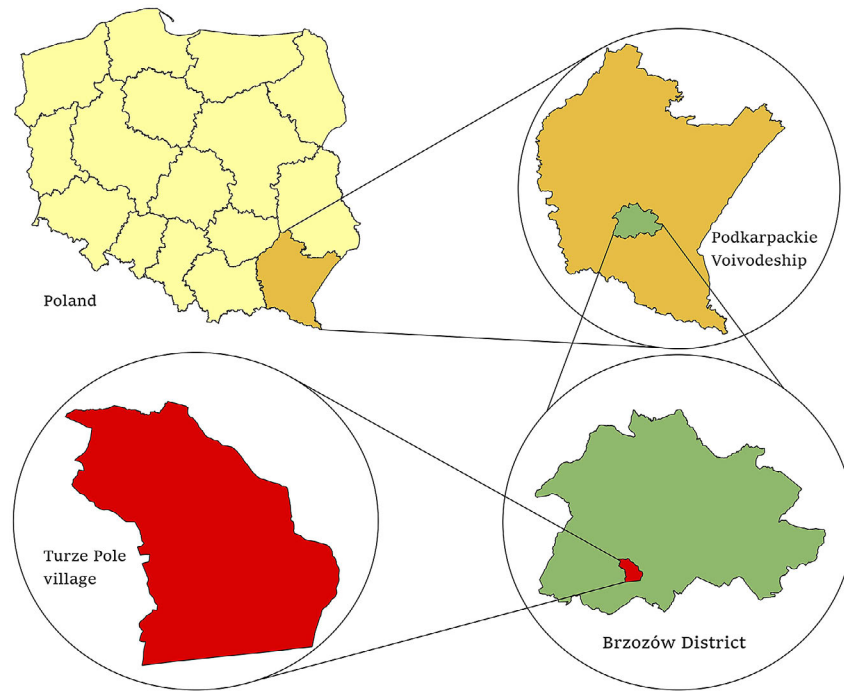


Figure 1. Location of the village of Turze Pole on the map of Poland, Subcarpathian voivodeship and the district of Brzozów; source: PRG (State Register of Borders), authors' elaboration

MATERIALS AND METHODS

For the needs of analyses, an orthophotomap generated during a photogrammetric flight by vertical take-off and landing (VTOL) tail-sitter Wingtra One Gen II was used. The price of the vehicle and the software in 2022 was about 270,000 PLN (about 60,625 EUR). The orthophotomap was compiled by the staff of the Subcarpathian Office of Land Surveying and Agricultural Areas (PBGiTR) in Rzeszów. Photographs were taken with SONY DSC-RX1RM2 cameras. Longitudinal and transverse overlap in photograph strips was 70%. Thirty photo points were established within the object. The total number of photos taken as a result of flights was 5362. The whole process of the data acquisition and processing took about 3 weeks. However, using the orthophotomaps and automated algorithms allowed to shorten the work time significantly in comparison to traditional surveying methods. All the photographs have been taken in good weather and lighting conditions. Some meteorological factors (e.g. fog or rain) may affect the quality of the photographs or make the flight impossible. Technical details about the equipment used and the orthophotomap produced are presented in Table 1 below. The trajectory of the flight, adjusted to the shape of the study area, is

Table 1. Information about the photogrammetric mission

RMS of reprojection error	0.65 px
RMS of distances to rays	0.0205 m
3D Error	0.01 m
Horizontal error	X: 0.0028 m; Y: 0.0057 m
Vertical error	0.0077 m
Flight altitude	120 m above ground level (constant)
Overlap of photographs	70% longitudinal overlap 70% transverse overlap
Ground sample distance	1.83 cm
Photograph dimensions	7952 × 5304 px 81.94 × 122.74 m
Photograph area	ca. 10 000 m ²
Flight speed	up to 16 m/s
Time Interval between Subsequent Photographs	ca. 1.5 s

Source: PBGiTR in Rzeszów.

presented in Figure 2. The precise coordinates of terrain vertices based on the orthophotomap were compared with the coordinates of object vertices recorded in the district geodetic and cartographic database maintained by the District Centre of Geodesic and Cartographic Records (PODGiK) in Brzozów.

The analysis covered objects from geodetic databases such as:

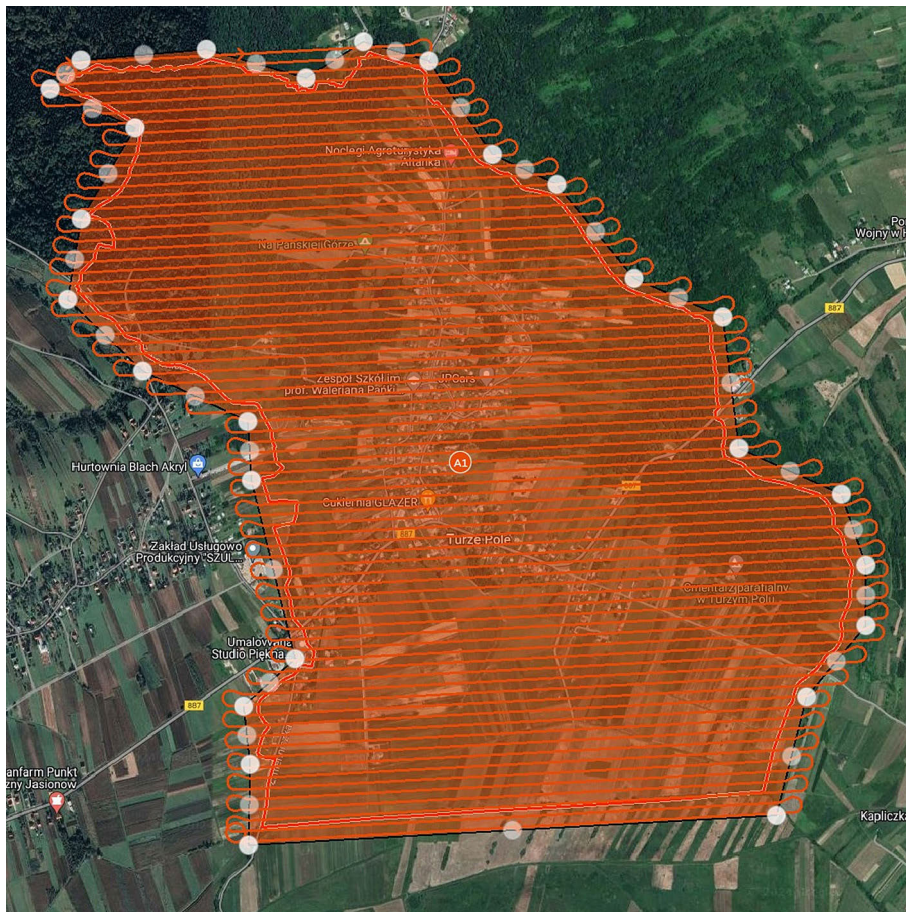


Figure 2. Trajectory of the flight; source: PBGiTR in Rzeszów

- land and buildings register – EGIB (real estate cadastre),
- topographic objects database – BDOT500,
- utilities network database – GESUT.

The EGIB, BDOT500 and GESUT databases contain classes of objects making up the base map of Poland. They are created in line with the guidance of Directive 2007/2/EC of the European Parliament and the Council of 14 March 2007, referred to as INSPIRE, and the Polish Act on the Infrastructure for Spatial Information of 4 March 2010 [61, 62]. According to the Regulation of the Minister of Development, Labour and Technology of 23 July 2021 concerning the topographic object database and the base map, the number of objects making up individual databases is: EGIB – 21 objects, BDOT500 – 80 objects and GESUT – 52 objects [63].

The number of objects analysed depended on the possibility of comparing the position of the objects and their orthophotomap-based counterparts. Thus, the main criterion for selecting the surveyed objects was their accessibility and

visibility. The analysis covered objects on and above land the specific features of which made it possible to locate their characteristic points precisely and unambiguously. In addition, it should be emphasised that certain classes of objects from EGIB, BDOT500, and GESUT databases were not present in the study area. Table 2 presents analysed classes of objects with a specification of the surveyed object vertices in each class.

The authors analysed the following number of object classes in individual databases: for EGIB – 1 object class, for BDOT500 – 16 object classes, and GESUT – 7 object classes. In total, 1158 pairs of geometrical object vertices were examined. For the EGIB database, the analysis only covered the vertices of stairs attached to buildings. Other objects were neglected since their outlines are usually located under the roof surface, which prevents the specification of the precise location of characteristic points. For building corners, the literature proposes a solution involving the use of a 3D model generated based on photogrammetric data. In view of the fact that the object of study was

Table 2. List of object classes covered by the analysis

Database	Class of objects	Number of objects
Egib	Stairs	31
BDOT500	Protective barrier	16
	Gateway	58
	Pavement	42
	Gate	43
	Other structure	77
	Other land use object	33
	Carriageway	70
	Curb	31
	Permanent fence	87
	Culvert	69
	Roadside ditch	62
	Stairs in a passageway	15
	Retaining wall	20
	Lawn	13
	Watercourse	20
	Still water	6
GESUT	Drain	27
	Lamp post	21
	Overground cables post	116
	Gas cabinet or container	16
	Water well	157
	Sewage well	83
	Power cabinet or container	45

the orthophotomap only, the above solution was not considered in this analysis. The following objects were selected from the BDOT500 database: protective barrier; gateway; pavement; gate; other structure; other land use object; carriageway; curb; retaining wall; permanent fence; culvert; canopy; roadside ditch; stairs in a passageway; lawn; watercourse, and still water. As regards the GESUT database, the following objects were qualified for analysis: drain, lamp post, gas cabinet or container, water well, sewage well, power cabinet or container, and overground cables post.

To ensure maximum objectivity of potential results and their practical application in land surveying, the assumptions of the analysis were based on accuracy standards in force in Poland, defined for individual objects from the geodetic databases EGIB, BOT500, and GESUT. The Regulation of the Minister of Development of 18 August 2020 on technical standards for topographic surveys and developing and transferring the results of these surveys to the state geodetic

and cartographic resource identified three groups of terrain details to satisfy the following accuracies with reference to the horizontal geodetic or measurement control network: 0.10 m – for group I terrain details; 0.30 m – for group II terrain details, and 0.50 m – for group III terrain details [64]. Terrain details from Group I include boundary markers and points, survey markers, and overground building structures and facilities, including overground elements of the utility network. Group II comprises earth structures and facilities and artificial water reservoirs, underground building structures and facilities, including underground utilities and land use elements including parks, green squares, lawns, playgrounds etc. Group III of terrain details includes the following objects: land use contours, soil pits, watercourses and water reservoirs, and forest divisions [64].

Surveying accuracy is defined by determining the point position error characterising measurements of various terrain details. According to the adopted assumption of the relative stability of orthophotomap accuracy, the examined accuracy of the vertices position of objects from geodetic databases was referenced to the position of their orthophotomap-based counterparts. The measure of surveying accuracy was the mean point position error calculated according to the following formula:

$$\sigma = \sqrt{\frac{\sum_{i=0}^n (X_{MZi} - X_{ORTOi})^2 + (Y_{MZi} - Y_{ORTOi})^2}{n}} \quad (1)$$

where: σ – mean point position error (RMSE, i.e. root-mean-square error), X_{MZi} , Y_{MZi} – XY coordinates of the i -th point according to the geodetic database, X_{ORTOi} , Y_{ORTOi} – XY coordinates of the i -th point according to the orthophotomap, n – number of observations [65].

To effectively calculate the mean vertices position errors for each of the surveyed object classes, a uniform computing algorithm was designed as a universal automated tool for use in various calculations in any research area. This proprietary algorithm, created using the “Model designer” device available in QGIS program, was adapted as a geoprocessing algorithm model supported by QGIS 3.32. Figure 3 shows a user view of the tool’s window.

To initiate the tool’s operation, relevant input data need to be indicated for the model, including the geometric points of object vertices from geodetic databases recorded in base maps and their

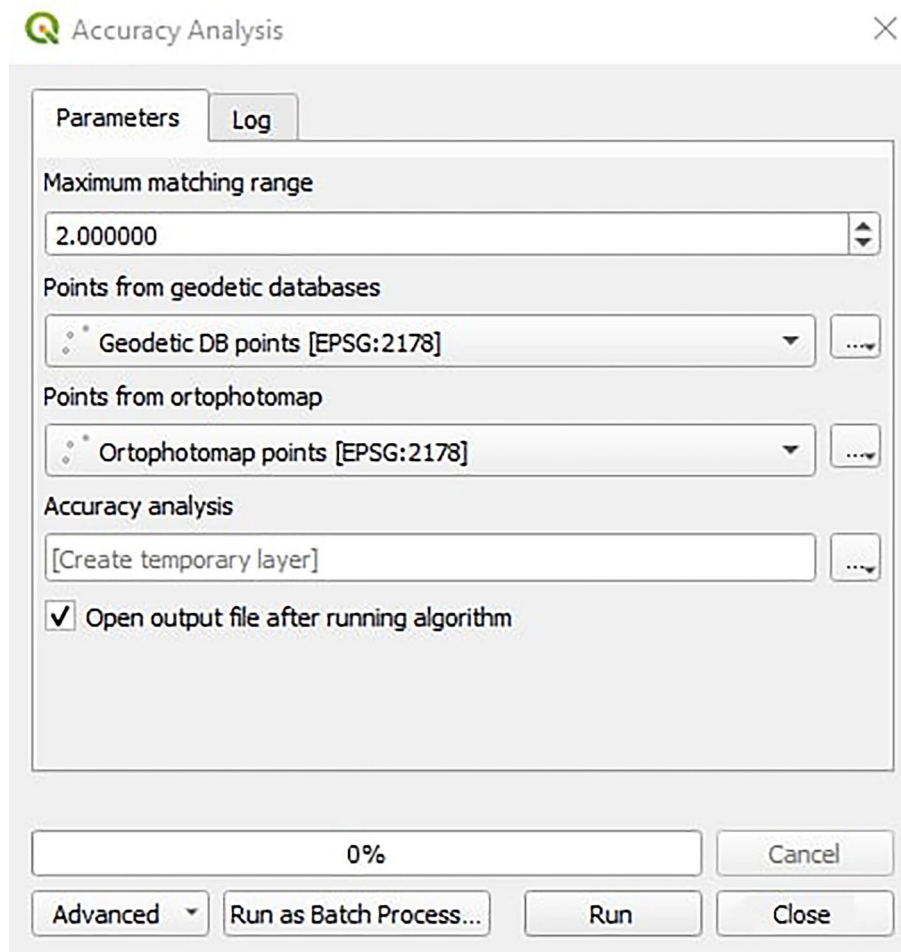


Figure 3. Window of the developed computing algorithm

orthophotomap-based counterparts. Depending on the assumptions, it is also necessary to indicate the search radius for the corresponding points of both input layers, point coordinates derived from the orthophotomap, and define the search buffers for potential pairs of points. Figure 4 contains a simplified flow chart illustrating the operation of the algorithm.

If the input is correct, the tool's operation can be initiated. First, the program preselects unique object vertices from geodetic databases forming potential pairs with points identified based on the orthophotomap. To ensure the reliability of the analysis, the points on the orthophotomap need to be identified and verified by an expert. Using automatic unsupervised classification methods may lead to misinterpretations due to similarities between the geometries of particular objects of the databases. If an unambiguous correlation between the vertices' position of the corresponding objects is achieved, subject to the maximum search distance, a pair of points is created. Unpaired points

are not further analysed. Next, the distance between points is calculated for individual pairs. The outcomes are compared with the applicable accuracy standards for each surveyed object class. Finally, the aggregated statistics regarding position differences of the corresponding vertices are computed for respective object classes.

RESULTS

Table 3 presents the results of the analysis of the vertices position accuracy for particular object classes, understood as root-mean-square error (RMS). The surveyed objects were classified according to the accuracy of terrain details determining the applicable surveying accuracy standard [64].

Yellow denotes the mean error in excess of the value indicated in the Regulation. Green denotes mean point position error meeting regulatory standards.

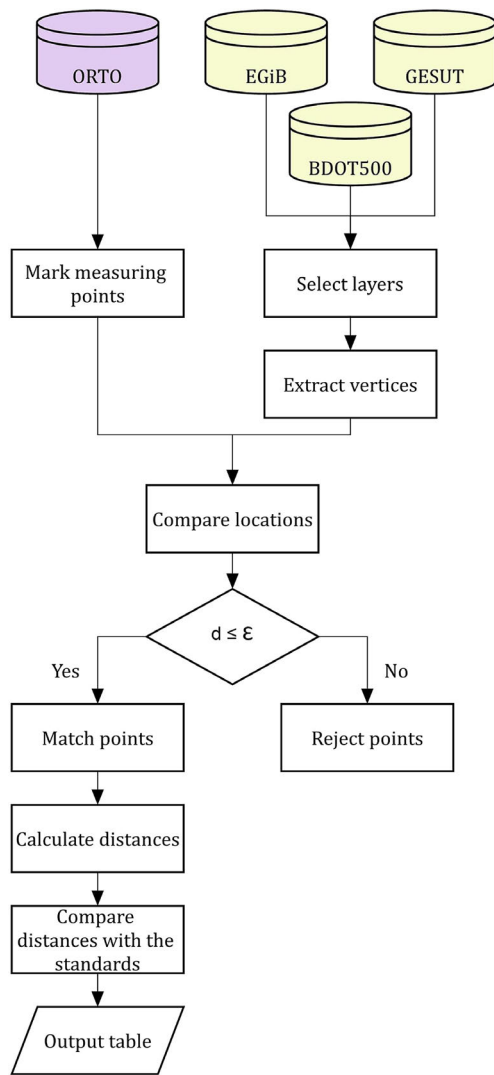


Figure 4. Operating principle of the automated computing algorithm for determining the mean vertices position error for individual classes of objects

In accuracy group III, the class of objects “watercourse” satisfies the required accuracy of 0.50 m. For “still water” the acceptable limit of error was insignificantly exceeded. However, it should be noted that the boundaries of water reservoirs and watercourses are subject to natural changes due to weather and anthropogenic factors etc. Three out of four surveyed object classes in accuracy group II, for which the standard is 0.30 m, do not meet the minimum accuracy requirements. The RMS was particularly high for ‘roadside ditch’ and ‘culvert’. Similar errors may be due to a technical correlation between facilities reflected by a topological relation. In contrast, the low error value for ‘lawn’ may be due to the common relationship between the geometrical vertices of lawns and the vertices of adjacent objects from a higher accuracy group such as pavement, carriageway or

curb. For accuracy group I in which 19 classes of objects were analysed, the maximum error limit of 0.10 m was achieved for nine classes. The highest mean error value was recorded for ‘other structure’. The result can reflect the variety of possible object types in this class due to which there are no unambiguous methods for measuring the geometry. The error value was also particularly high for ‘power cabinet or container’. This case is discussed in detail hereinafter.

Figure 5 shows mean point position errors for the surveyed object classes from accuracy groups, specifying the acceptable limit of error for surveys. The blue circle denotes the area of acceptable position errors for objects from group I of terrain details (0.10 m), the orange circle – objects from group II of terrain details (0.30 m), and green marks the required surveying accuracy for group III of terrain details. The predominant part of the surveyed object classes, including 17 out of 19 surveyed object classes from the highest accuracy group, does not exceed the RMSE of 0.20 m. Despite exceeding applicable limits, most likely due to the presence of geometric data acquired using methods not compliant with the contemporary standards and local constraints on orthophotomap accuracy, spatial consistency between the geodetic databases and the orthophotomap content can be seen at the general analysis level. This may be a basic assumption for the concept of delimiting potential areas in need of updating the contents of numerical maps as the local extremes of object vertices position errors with reference to the orthophotomap.

The aggregation of accuracy characteristics according to object classes using the mean error function is only a general indicator of the expected surveying accuracy. To specify the results, the distribution of position errors of the surveyed vertices for individual object classes was analysed. For each of the surveyed object classes, Table 4 gives a cumulative percentage share of vertices achieving individual position error limits in the overall number of object vertices representing the specific class. Green denotes the percentage of vertices with position errors equal to the standard applicable to the relevant accuracy group or lower. The red values point to the occurrence of objects with position accuracy not satisfying respective standards. The acceptable position error limit is, in addition, marked by a red line.

Only three out of 24 surveyed object classes (pavement, gas cabinet or container, and lawn)

Table 3. Analysis of analysed object vertices position accuracy

Group I		Group II		Group III	
Accuracy standard: 0.100 m		Accuracy standard: 0.300 m		Accuracy standard: 0.500 m	
Object	RMS [m]	Object	RMS [m]	Object	RMS [m]
Protective barrier	0.054	Other land use object	0.312	Watercourse	0.383
Gateway	0.123	Culvert	0.423	Still water	0.526
Pavement	0.037	Roadside ditch	0.452		
Gate	0.107	Lawn	0.070		
Other structure	0.225				
Carriageway	0.049				
Drain	0.096				
Curb	0.048				
Lamp post	0.157				
Retaining wall	0.114				
Permanent fence	0.097				
Stairs in a passageway	0.079				
Stairs	0.143				
Overground cables post	0.166				
Gas cabinet or container	0.117				
Water well	0.151				
Sewage well	0.096				
Power cabinet or container	0.221				

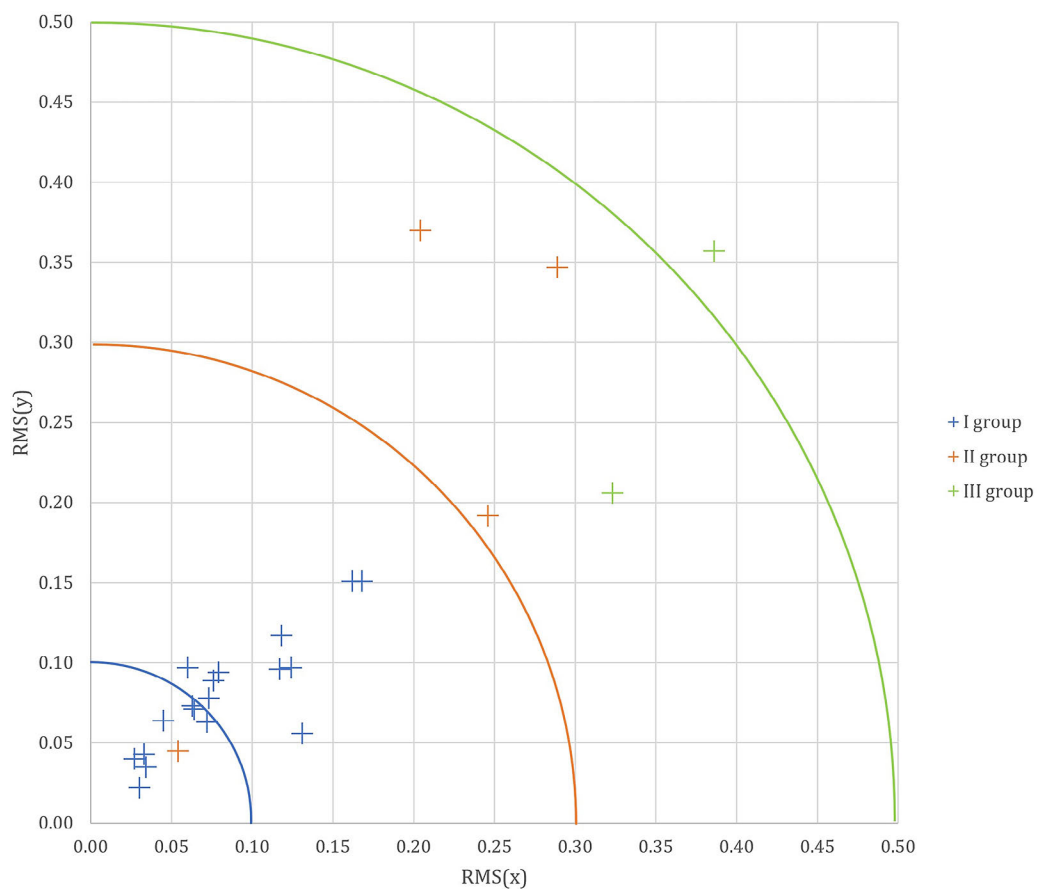


Figure 5. Mean position errors of the surveyed object classes in the geodetic databases EGiB, BDOT500, and GESUT with reference to their orthophotomap-based counterparts

Table 4. The cumulative percentage of position error limits in relation to the orthophotomaps for the surveyed objects from geodetic databases

Error [m]:	0.05	0.10	0.15	0.20	0.30	0.40	0.50	0.60	0.80	1.00
Protective barrier	6%	81%	94%	100%	100%	100%	100%	100%	100%	100%
Gateway	9%	40%	71%	79%	93%	100%	100%	100%	100%	100%
Pavement	14%	86%	100%	100%	100%	100%	100%	100%	100%	100%
Gate	0%	35%	63%	88%	100%	100%	100%	100%	100%	100%
Other structure	0%	8%	32%	53%	77%	88%	99%	99%	100%	100%
Carriageway	10%	79%	97%	99%	100%	100%	100%	100%	100%	100%
Drain	4%	59%	89%	93%	96%	100%	100%	100%	100%	100%
Curb	29%	87%	90%	100%	100%	100%	100%	100%	100%	100%
Lamp post	0%	38%	52%	71%	90%	100%	100%	100%	100%	100%
Permanent fence	0%	39%	76%	90%	99%	100%	100%	100%	100%	100%
Stairs	3%	45%	81%	87%	94%	97%	97%	97%	100%	100%
Stairs in a passageway	0%	67%	87%	93%	100%	100%	100%	100%	100%	100%
Overground cables post	1%	21%	43%	72%	89%	98%	99%	99%	100%	100%
Water well	9%	43%	66%	78%	92%	97%	99%	99%	100%	100%
Sewage well	2%	55%	78%	90%	98%	100%	100%	100%	100%	100%
Power cabinet or container	4%	31%	49%	76%	89%	91%	93%	96%	98%	100%
Gas cabinet or container	0%	40%	100%	100%	100%	100%	100%	100%	100%	100%
Retaining wall	0%	45%	65%	75%	100%	100%	100%	100%	100%	100%
Other land use object	0%	6%	27%	48%	70%	85%	91%	91%	94%	97%
Culvert	0%	13%	23%	30%	46%	65%	77%	87%	91%	96%
Roadside ditch	2%	2%	10%	18%	39%	52%	69%	79%	95%	98%
Lawn	0%	38%	92%	100%	100%	100%	100%	100%	100%	100%
Watercourse	0%	0%	0%	15%	55%	65%	80%	90%	95%	100%
Still water	0%	0%	0%	33%	33%	50%	50%	50%	83%	100%
Total:	4%	37%	60%	74%	86%	92%	96%	97%	99%	100%

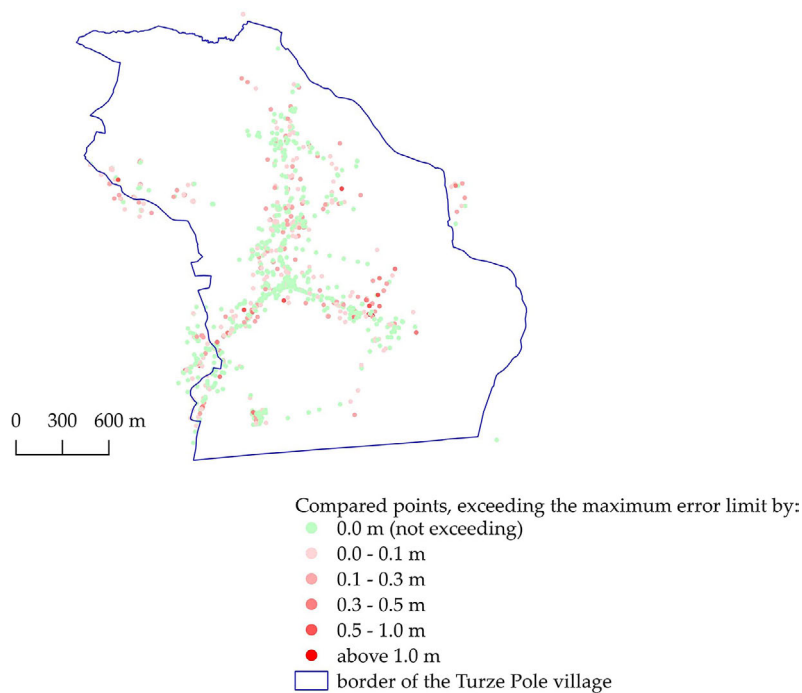


Figure 6. Distribution of vertices errors of objects in geodetic databases in reference to the orthophotomap

contained no objects positioned in reference to the orthophotomap beyond the applicable standard. For ten classes of objects from various groups, more than 50% of the surveyed objects achieved the accuracy standard in reference to the orthophotomap. Simultaneously, for 18 classes of objects, including 15 classes from the highest accuracy group, more than 75% of the surveyed objects featured the position error not exceeding the applicable limit increased by 0.10 m. Therefore, the relatively rare cases of exceeded acceptable position error limit by more than 0.30 m, constituting about 14% of the analysed samples, should be considered potential local signs of obsolescence of the contents of geodetic databases which require special verification. The spatial distribution of values of the calculated errors in the studied village is presented in Figure 6.

A relatively high correspondence between the position of the surveyed vertices and the orthophotomap was recorded in areas adjacent to the main transport axes of the village and concentrated around their junction, in the central part of the village. The noticeable clusters of points exceeding the applicable maximum surveying error are mostly located in the southwest and southeast of the village. To maximise objective assessment of the location of clusters of points with the highest error values in reference to the orthophotomap,

the output data file was visualised as a heatmap, with the visibility of the surveyed vertices limited to points exceeding the position error for the given accuracy group by more than 0.30 m and taking as weight $\varepsilon-0.30$, where ε denotes the difference between the position of the point on the numerical map and its position on the orthophotomap. The cartographic visualisation prepared using this method is presented in Figure 7.

The light-coloured areas in the figure above are clusters of points with position discrepancies between the geodetic database and the orthophotomap exceeding 0.30 m. This cartographic visualisation method facilitates the preliminary delimitation of areas requiring special control and potential correction of the measurement of terrain details. The area with the highest concentration of potential position errors, as seen in the figure above, is additionally depicted as a detail indicating the location of the surveyed vertices showing a position mismatch and the value exceeding the acceptable surveying error limit.

A general analysis of the spatial distribution of object position mismatch between the geodetic databases and the orthophotomap with documented high accuracy can provide initial information on areas potentially requiring verification and updating of terrain detail measurements. A detailed analysis of the accuracy of the geodetic survey

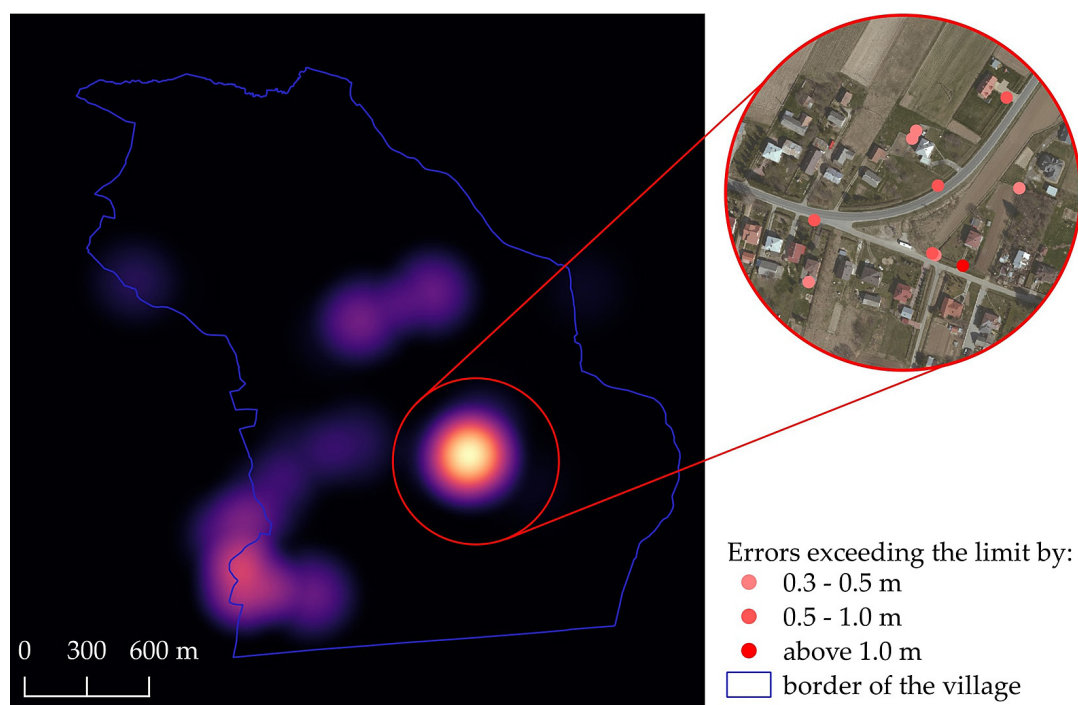
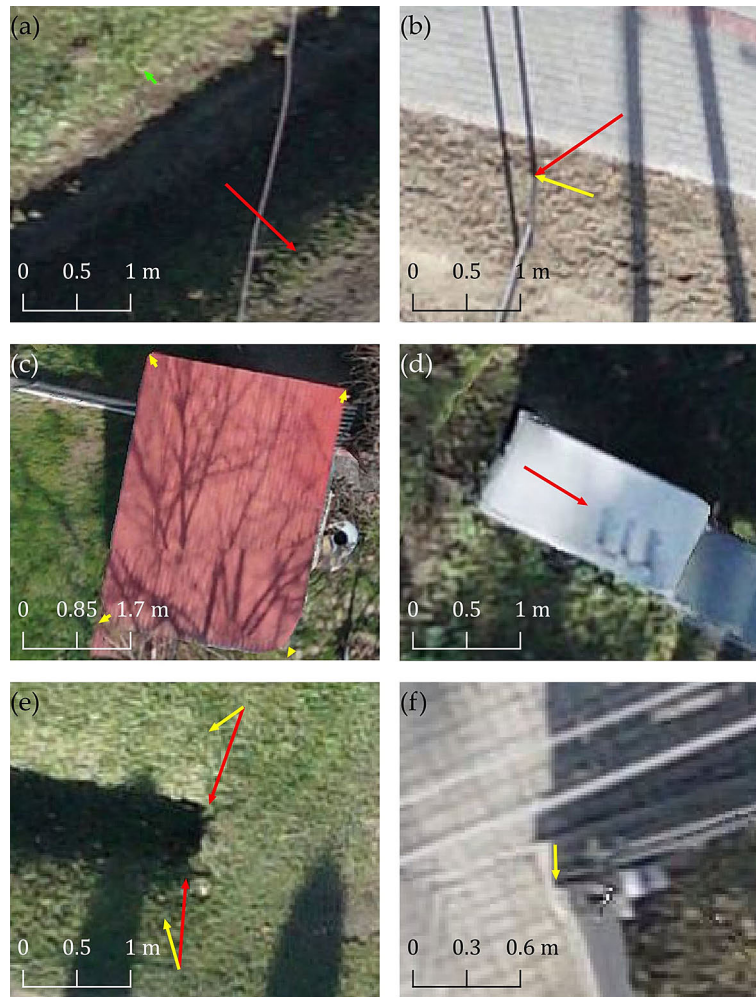


Figure 7. Heatmap of points with position discrepancies exceeding 0.30 m, including details representing locations with a particularly high concentration of potential errors



RMSE vectors:
 → equal to the limit or less
 → exceeding the limit by 0.0-0.5 m
 → exceeding the limit by more than 0.5 m

Figure 8. Examples of identified differences in the position of object vertices in reference to their position on the orthophotomap: (a) roadside ditch; (b) other land use object – billboard; (c) other building structure; (d) power cabinet or container; (e) culvert, roadside ditch; (f) permanent fence

and the numerical map requires consideration of the peculiar features of the individual object classes and the directions and values of the observed position deviations. Based on the results calculated using the algorithm, the parameters of the position error vectors were visualised. Selected examples of discrepancies between the position of object vertices from different classes and the position of their counterparts on the orthophotomap are illustrated in Figure 8.

Insignificant discrepancies between object vertices' position documented in geodetic databases and their location on the orthophotomap are usually natural, and stem, among other things, from the limited accuracy of land surveying

methods and orthophotomap errors. However, assuming a sufficiently high quality of the orthophotomap, documented by an accuracy analysis using checkpoints with measured coordinates, position differences significantly exceeding the potential outcome of land survey and orthophotomap errors should be considered as local indicators of inaccuracy or obsolescence of the numerical map contents. However, the final determination of the need to update the content of the geodetic databases should be preceded by an expert assessment, considering specific features of individual object types and real possibilities of optimising accuracy using available surveying techniques. Examples shown in the above

figure, relating to objects within the study area, illustrate the varying degrees of local disturbance to the accuracy and timeliness of the geodetic numerical map in terms of objects from different classes. Examples (a) and (e) refer to the inter-related objects ‘roadside ditch’ and ‘culvert’. The high value of position error of the ditch boundaries (approx. 1 m) and the location of the existing vertex near the ditch bottom implies a need for remeasurement, either due to a defect of the previous measurement or terrain changes. As ‘roadside ditch’ and ‘culvert’ belong to accuracy group II with an acceptable surveying error of 0.30 m, it is possible to measure the objects on the basis of a suitably accurate orthophotomap [60].

Cases (b) and (f) involve vertically positioned objects. Correct identification of their location on the basis of an orthophotomap requires the use of high-precision photogrammetric materials and particularly careful identification of key object vertices, which are difficult to locate due to, among other things, their small size and interference by shadows and objects limiting visibility. However, the presented examples such as a billboard (b) and a fence (f), make it possible to unambiguously detect the incorrect position of objects on the numerical map.

Case (c), the so-called ‘other structure’ (e.g. garage other than a building, canopy, gazebo), does not make it possible to clearly identify an error or obsolescence in the contents of the numerical map. Despite demonstrating significant (from 0.18 m to 0.37 m) differences in the position of the vertices between the numerical map and the orthophotomap, here attention should be paid to the high risk of mislabelling object vertices when analysing the orthophotomap. This is because photogrammetric imaging only makes it possible to identify the corners of the object’s canopy, the projection of which may not coincide with the outline of the overground part subject to land surveys. In addition, the possibility of accurately delimiting the object’s outline using an orthophotomap has been significantly reduced due to the presence of so-called artefacts, which are a relatively common consequence of errors in generating orthophotomap.

A particularly clear example of an obsolete geodetic numerical map was identified in case (d), concerning a power cabinet. According to current assumptions, a GESUT database object with point geometry should reflect the geometric centre of the actual terrain detail. The recorded

offset of approximately 0.70 m explicitly implies terrain changes, an incorrect geodetic survey or a numerical map preparation error. Evidence of outdated databases may be the fact that the power cabinet in the immediate vicinity of the surveyed object is not shown. The position error can also result from the misplacement of a point object at the junction between the underground conductor and the power cabinet, away from the geometric centre of the object.

Summing up the result of the analyses carried out, it is necessary to confirm the assumption that a high-resolution orthophotomap with sufficiently high accuracy can be used as a practical tool to efficiently determine the urgency of potential updates to the numerical map and indicate priority objects and areas requiring correction. However, special attention should be paid to the possible causes of discrepancies and consideration should be given to potential imperfections and constraints of the photogrammetric survey. It is also possible to use the orthophotomap for the direct acquisition of numerical map objects, subject to adequate surveying accuracy. The current regulation requires the surveying supervisor to ensure the accuracy of the transmitted measurements as required for each accuracy group [60]. However, the legislator does not limit the range of permissible measuring instruments or techniques, so the use of UAVs in land surveys conducted in Poland is not against the law [64].

DISCUSSION

The use of UAV technology in acquiring terrain information is a useful alternative to conventional land surveying and GNSS surveys. The possibility of up-to-date, large-area and comprehensive surveys in a short time is a particular advantage of this technology, which contributes to a dynamic development of uses of unmanned aerial vehicles in surveying work. The analysis showed that it is reasonable to use UAV technology for creating and updating the geodetic databases EGIB, BDOT500 and GESUT based on a high-quality orthophotomap, provided that the accuracy of the position of the retrieved objects is first verified. Pyka also represents this view, who points out that the accuracy verification procedure is a necessary activity on the part of the surveying manager due

to the obligation to ensure accuracy as defined by law [43, 64].

Comparing the number of objects comprising the base map with the number of elements analysed, it can be concluded that a significant proportion of objects present in geodetic databases cannot be extracted from the orthophotomap. These constraints, in particular, due to the fact that certain elements are obscured, and underground objects are not visible, reduce the functionality of the orthophotomap as a source for acquiring numerical map objects. To expand the range of retrievable objects, researchers point, among other solutions, to the possibility of using a 3D model generated from oblique images. In their study, Karabin et al. present the possibility of using the 3D model to measure building corners covered by roofs and hence not visible on the orthophotomap [55]. Such a solution would also allow to acquire extensive three-dimensional data, which would be a valuable data source in the potential process of creating a 3D cadastre in Poland. The use of large-scale photogrammetric views, covering an increasing number of areas, could then be one of the fundamental terrain data sources.

The analysis also revealed insufficient validity of the base map, due to dynamic spatial transformations taking place. Geodetic database validity, which is a widely discussed subject, has also been documented by other authors [55, 56]. Maintaining sufficient validity of numerical maps is a highly complex problem. Indeed, to ensure maximum conformity of the geodetic databases with the actual state of affairs would require a geodetic inventory of any new or modified terrain detail. This rule, being commonly followed for cadastral objects and utility networks, does not in practice cover all terrain changes. An alternative approach could include a regular campaign to update the contents of geodetic databases based on field verification and measurements of terrain details. However, it should be noted that such practices would be potentially expensive. The use of UAV technology can significantly reduce labour costs, replacing time-consuming field verification of the content's accuracy of geodetic databases and providing an effective tool for delimiting priority areas in need of updating. Also, eliminating the need to survey some terrain details, including ditches, water reservoirs and watercourses from accuracy groups II and III, which are often characterised by limited access,

may contribute to minimising the time and cost of updating geodetic databases while maintaining satisfactory work efficiency.

The dynamic development of technology, both in terms of the performance and functionality of UAVs and in the area of modern surveying tools and methods, makes the case for undertaking steps to integrate various data sources in acquiring terrain information. The constraints on the uses of orthophotomap demonstrated in the course of this study can be supplemented, for instance, by measurements using a LIDAR sensor, the usefulness of which in surveying, including cadastral surveys, is highlighted by Šafář et al. [59] and He and Li [66].

CONCLUSIONS

UAV technology enables efficient acquisition of relatively accurate and specific terrain information. The possibility of making wide-area aerial photogrammetric surveys at low costs of flights and data processing legitimises the use of UAVs for geodesic and cartographic tasks, including the acquisition of information on the current state of terrain details to be inventoried as objects of geodetic databases.

The research, which involved, among other things, comparing the position of the vertices of numerical map objects with their counterparts identified on a high-accuracy orthophotomap, showed that a significant proportion of the objects surveyed do not meet the accuracy standards required by the legislator. Where acceptable position errors are slightly exceeded, the possibility to unambiguously identify outdated or incorrectly entered objects is limited due to the inherent imperfection of the orthophotomap and its interpretation. However, numerous observed discrepancies exceeding the applicable measurement uncertainty limits of more than 0.30 m may be considered a potential manifestation of obsolescence or substantive defects of geodetic numerical maps, which corroborates the need for updating the spatial information resource.

The automated computing algorithm and transparent cartographic visualisation methods have contributed to the creation of a versatile tool, providing for efficient pre-validation of numerical maps and delimitation of priority areas for verification and potential updates. The proposed method may significantly support various studies on

cadastre validity, conducted for scientific or practical purposes. Using UAV-based measurements and automated computing tools reduces the time of data processing and provides high reliability of the outcomes. A detailed case study of the actual area confirmed the tool's assumed effectiveness. Simultaneously, attention should be drawn to the constraints on using the orthophotomap as a reference for the position of geodetic database objects. A particularly vital problem is the inability to identify elements obscured by other objects, as well as underground objects and objects with vertical geometry, such as poles and smaller fences, among other items. As a partial solution to this problem, literature cites the use of metric oblique imagery and the implementation of alternative data sources, including laser scanning techniques.

In authors' opinion, research into the effectiveness of alternative methods for geodetic and cartographic tasks is necessary for optimising spatial information management methodologies. Indeed, the implementation of documented high-performance solutions enabling the partial elimination of time-consuming work in favour of methods that ensure high-quality outcomes while reducing labour costs, is an integral part of civilisational progress, as observed, among other areas, in the field of land surveying and cartography.

REFERENCES

- Ćwiąkała P., Gruszczyński W., Stoch T., Puniach E., Mrocheń D., Matwij W., Matwij K., Nędzka M., Sopata P., Wójcik A. UAV Applications for determination of land deformations caused by underground mining. *Remote Sens.* 2020, 12, 1733. <https://doi.org/10.3390/rs12111733>
- Borowik G., Koźdoń-Dębecka M., Strzelecki S. Movable Observation Used by Television Drone Pilots: Efficiency of Aerial Filming Regarding the Quality of Completed Shots. *Electron.* 2022, 11, 3881. <https://doi.org/10.3390/electronics11233881>
- Kovanič E., Topitzer B., Peťovský P., Blišťan P., Gergel'ová M.B., Blišťanová M. Review of Photogrammetric and Lidar Applications of UAV. *Appl. Sci.* 2023, 13, 6732. <https://doi.org/10.3390/app13116732>
- Sestras P., Bilaşco Ş., Roşca S., Dudic B., Hysa A., Spalević V. Geodetic and UAV monitoring in the sustainable management of shallow landslides and erosion of a susceptible urban environment. *Remote Sens.* 2021, 3, 385. <https://doi.org/10.3390/rs13030385>
- Gerke M., Przybilla H.-J. Accuracy analysis of photogrammetric UAV image blocks: Influence of onboard RTK-GNSS and cross flight patterns. *Photogramm. Fernerkund. Geoinf.* 2016, 14, 17–30. <https://doi.org/10.1127/pfg/2016/0284>
- Malihi S., Valadan Zoej M.J., Hahn M. Large-scale accurate reconstruction of buildings employing point clouds generated from UAV imagery. *Remote Sens.* 2018, 10, 1148. <https://doi.org/10.3390/rs10071148>
- Marmanis D., Schindler K., Wegner J.D., Galiani S., Datcu M., Stilla U. Classification with an edge: Improving semantic image segmentation with boundary detection. *ISPRS J. of Photogramm. and Remote Sens.* 2018, 135, 158–172 <https://doi.org/10.1016/j.isprsjprs.2017.11.009>
- Ružić I., Benac Č., Jovančević S.D., Radišić M. The Application of UAV for the analysis of geological hazard in Krk Island, Croatia, Mediterranean Sea. *Remote Sens.* 2021, 13, 1790. <https://doi.org/10.3390/rs13091790>
- Boccardo P., Chiabrando F., Dutto F., Tonolo F.G., Lingua A. UAV deployment exercise for mapping purposes: evaluation of emergency response applications. *Sens.* 2015, 15, 15717–15737. <https://doi.org/10.3390/s150715717>
- Tokarczyk P., Leitao J.P., Rieckermann J., Schindler K., Blumensaat F. High-quality observation of surface imperviousness for urban runoff modelling using UAV imagery. *Hydrol. Earth Syst. Sci.* 2015, 19, 4215–4228. <https://doi.org/10.5194/hess-19-4215-2015>
- Skondras A., Karachaliou E., Tavantzis I., Tokas N., Valari E., Skalidi I., Bouvet G.A., Stylianidis E. UAV mapping and 3D modeling as a tool for promotion and management of the urban space. *Drones* 2022, 6, 115. <https://doi.org/10.3390/drones6050115>
- Nex F., Remondino F. UAV for 3D mapping applications: A review. *Appl. Geomat.* 2014, 6, 1–15. <https://doi.org/10.1007/s12518-013-0120-x>
- Fernandez Galarreta J., Kerle N., Gerke M. UAV-based urban structural damage assessment using object-based image analysis and semantic reasoning. *Nat. Hazards Earth Syst. Sci.* 2015, 15, 1087–1101. <https://doi.org/10.5194/nhess-15-1087-2015>
- Vetrivel A., Gerke M., Kerle N., Vosselman G. Segmentation of UAV-based images incorporating 3D point cloud information. *Int. Arch. Photogramm. Remote Sens. Spatial Inf. Sci.* 2015, XL-3/W2, 261–268. <https://doi.org/10.5194/isprsarchives-XL-3-W2-261-2015>
- Vetrivel A., Gerke M., Kerle N., Vosselman G. Identification of structurally damaged areas in airborne oblique images using a visual-Bag-of-Words approach. *Remote Sens.* 2016, 8(3), 231. <https://doi.org/10.3390/rs8030231>

16. Hoffmann H., Nieto H., Jensen R., Guzinski R., Zarco-Tejada P., Friborg T. Estimating evaporation with thermal UAV data and two-source energy balance models. *Hydrol. Earth Syst. Sci.*, 2016, 20, 697–713. <https://doi.org/10.5194/hess-20-697-2016>
17. Colomina I., Molina P. Unmanned aerial systems for photogrammetry and remote sensing: A review. *ISPRS J. Photogramm. Remote Sens.* 2014, 92, 79–97. <https://doi.org/10.1016/j.isprsjprs.2014.02.013>
18. Mesas-Carrascosa F.J., Notario-García M.D., de Larriva J.E.M., de la Orden M.S., Porrás A.G.-F. Validation of measurements of land plot area using UAV imagery. *Int. J. Appl. Earth Obs. Geoinform.* 2014, 33, 270–279. <https://doi.org/10.1016/j.jag.2014.06.009>
19. Fernández-Hernandez J., González-Aguilera D., Rodríguez-González P., Mancera-Taboada J. Image-based modelling from unmanned aerial vehicle (UAV) photogrammetry: An effective, low-cost tool for archaeological applications. *Archaeometry* 2015, 57, 128–145. <https://doi.org/10.1111/arc.12078>
20. Pajares G. Overview and current status of remote sensing applications based on unmanned aerial vehicles (UAVs). *Photogramm. Eng. Remote Sens.* 2015, 81, 281–330. <https://doi.org/10.14358/PERS.81.4.281>
21. Orihuela A., Molina-Fajardo M.A. UAV photogrammetry surveying for sustainable conservation: The case of Mondújar Castle (Granada, Spain). *Sustain.* 2021, 13, 24. <https://doi.org/10.3390/su13010024>
22. Du S., Zhang Y., Qin R., Yang Z., Zou Z., Tang Y., Fan C. Building change detection using old aerial images and new LiDAR data. *Remote Sens.* 2016, 8(12), 1030. <https://doi.org/10.3390/rs8121030>
23. Zhu J.S., Sun K., Jia S., Li Q.Q., Hou X.X., Lin W.D., Liu B.Z., Qiu G.P. Urban traffic density estimation based on ultra-high-resolution UAV video and deep neural network. *IEEE J. Sel. Top. Appl. Earth Obs. Remote Sens.* 2018, 11, 4968–4981. <https://doi.org/10.1109/JSTARS.2018.2879368>
24. Ren H., Zhao Y., Xiao W., Hu Z. A review of UAV monitoring in mining areas: current status and future perspectives. *Int. J. Coal. Sci. Technol.* 2019, 6, 320–333. <https://doi.org/10.1007/s40789-019-00264-5>
25. Yao H., Qin R., Chen X. Unmanned aerial vehicle for remote sensing applications—A review. *Remote Sens.* 2019, 11, 1443. <https://doi.org/10.3390/rs11121443>
26. Wu B. Photogrammetry for 3D Mapping in Urban Areas. In: Shi W., Goodchild M.F., Batty M., Kwan M.P., Zhang A. *Urban informatics. The Urban Book Series.* Springer, Singapore 2021. https://doi.org/10.1007/978-981-15-8983-6_23
27. Ahmed F., Mohanta J.C., Keshari A., Yadav P.S. Recent advances in unmanned aerial vehicles: A review. *Arab. J. Sci. Eng.* 2022, 47, 7963–7984. <https://doi.org/10.1007/s13369-022-06738-0>
28. Beselly S.M., van der Wegen M., Grueters U., Reyns J., Dijkstra J., Roelvink D. Eleven years of mangrove–mudflat dynamics on the mud volcano-induced prograding delta in East Java, Indonesia: Integrating UAV and Satellite Imagery. *Remote Sens.* 2021, 13, 1084. <https://doi.org/10.3390/rs13061084>
29. Sturdivant E.J., Lentz E.E., Thieler E.R., Farris A.S., Weber K.M., Remsen D.P., Miner S., Henderson R.E. UAS-SfM for Coastal Research: Geomorphic Feature Extraction and Land Cover Classification from High-Resolution Elevation and Optical Imagery. *Remote Sens.* 2017, 9(10), 1020. <https://doi.org/10.3390/rs9101020>
30. Congress S.S.C., Puppala A.J., Lundberg C.L. Total system error analysis of UAV-CRP technology for monitoring transportation infrastructure assets. *Eng. Geol.* 2018, 247, 104–116. <https://doi.org/10.1016/j.enggeo.2018.11.002>
31. Guan S., Zhu Z., Wang G.A. Review on UAV-based remote sensing technologies for construction and civil applications. *Drones* 2022, 6, 117. <https://doi.org/10.3390/drones6050117>
32. Crommelinck S., Bennett R., Gerke M., Nex F., Yang M.Y., Vosselman G. Review of automatic feature extraction from high-resolution optical sensor data for UAV-based cadastral mapping. *Remote Sens.* 2016, 8, 689. <https://doi.org/10.3390/rs8080689>
33. Alemie B.K., Bennett R.M., Zevenbergen J. Evolving urban cadastres in Ethiopia: The impacts on urban land governance. *Land Use Policy* 2015, 42, 695–705. <https://doi.org/10.1016/j.landusepol.2014.10.001>
34. Jazayeri I., Rajabifard A., Kalantari M. A geometric and semantic evaluation of 3D data sourcing methods for land and property information. *Land Use Policy* 2014, 36, 219–230. <https://doi.org/10.1016/j.landusepol.2013.08.004>
35. Turner D., Lucieer A., De Jong S.M. Time series analysis of landslide dynamics using an unmanned aerial vehicle (UAV). *Remote Sens.* 2015, 7(2), 1736–1757. <https://doi.org/10.3390/rs70201736>
36. Wallace L., Lucieer A., Malenovský Z., Turner D., Vopěnka P. Assessment of forest structure using two UAV techniques: A comparison of airborne laser scanning and structure from motion (SfM) point clouds. *Forests* 2016, 7, 62. <https://doi.org/10.3390/f7030062>
37. Ožóg K. The use of unmanned aerial vehicles for the assessment of land boundaries accuracy. *J. Water Land Dev.* 2019, 45, 94–99. <https://doi.org/10.24425/jwld.2020.133050>
38. Stöcker C., Koeva M.N., Nkerabigwi P., Zevenbergen J.A. UAV Technology: Opportunities to Support the Updating Process of the Rwandan Cadastre. In: *FIG Working Week 2020, Amsterdam, Netherlands, 2020.* https://www.fig.net/resources/proceedings/fig_proceedings/fig2020/papers/ts07h/

- TS07H_stocker_koeva_et_al_10290.pdf. (Accessed: 04.12.2023)
39. Stöcker C., Nex F., Koeva M., Gerke M. High-quality UAV-based orthophotos for cadastral mapping: guidance for optimal flight configurations. *Remote Sens.* 2020, 12, 3625. <https://doi.org/10.3390/rs12213625>
 40. Stöcker C., Bennett R., Koeva M., Nex F., Zevenbergen J. Scaling up UAVs for land administration: Towards the plateau of productivity. *Land Use Policy* 2022, 114, 105930, <https://doi.org/10.1016/j.landusepol.2021.105930>
 41. Doroż A., Bożek P., Maciąg K., Maciąg M., Leń P. Zastosowanie bezzałogowych statków powietrznych w pozyskiwaniu materiałów fotogrametrycznych na potrzeby realizacji kompleksowych prac scaleniowych [The use of UAV in the acquisition of photogrammetric materials for the implementation of land consolidation]. *Prz. Geod.* 2023, 6, 26–29. <https://doi.org/10.15199/50.2023.06.2> (In Polish)
 42. Ajayi O.G., Oruma E. On the applicability of integrated UAV photogrammetry and automatic feature extraction for cadastral mapping. *Adv. Geod. Geoinf.* 2022, 71, 1, e19. <https://doi.org/10.24425/gac.2022.141172>
 43. Pyka K. Prawne, techniczne i społeczne aspekty pomiarów fotogrametrycznych [Legal, technical and social aspects of photogrammetric measurements]. *Prz. Geod.* 2016, 1, 8–12. <https://doi.org/10.15199/50.2016.11.1> (In Polish)
 44. Brach M., Gąsior J. Przydatność niskokosztowego bezzałogowego statku powietrznego do weryfikacji wybranych elementów mapy zasadniczej [Usage of the low cost unmanned aerial vehicle in the master map verification process for selected classes]. *Prz. Geod.* 2022, 1, 32–35 <https://doi.org/10.15199/50.2022.1.4> (In Polish)
 45. Van Canh L., Xuan Cuong C., Quoc Long N., Thi Thu Ha L., Trung Anh T., Bui, X.-N. Experimental Investigation on the Performance of DJI Phantom 4 RTK in the PPK Mode for 3D Mapping Open-Pit Mines. *J. Pol. Miner. Eng. Soc.* 2020, 1(2), 65–74. <https://doi.org/10.29227/IM-2020-02-10>
 46. Feng Q., Liu J., Gong J. UAV Remote Sensing for Urban Vegetation Mapping Using Random Forest and Texture Analysis. *Remote Sens.* 2015, 7, 1074–1094. <https://doi.org/10.3390/rs70101074>
 47. Barlow J., Gilham J., Ibarra Cofrã I. Kinematic analysis of sea cliff stability using UAV photogrammetry. *Int. J. Remote Sens.* 2017, 38, 2464–2479. <https://doi.org/10.1080/01431161.2016.1275061>
 48. Borkowski A.S. A Literature review of BIM definitions: Narrow and broad views. *Technol.* 2023, 11, 176. <https://doi.org/10.3390/technologies11060176>
 49. Borkowski A.S. Evolution of BIM: epistemology, genesis and division into periods. *J. Inf. Technol. Constr.* 2023, 28, 646–661. <https://doi.org/10.36680/j.itcon.2023.034>
 50. Borkowski A.S. Experiential learning in the context of BIM[J]. *STEM Educ.* 2023, 3(3), 190–204. <https://doi.org/10.3934/steme.2023012>
 51. Borkowski A.S., Firlńska S.A. Modelling of transmission infrastructure in BIM technology. *Prz. Elektrotech.* 2022, 98, 12, 133–135. <https://doi.org/10.15199/48.2022.12.33>
 52. Borkowski A.S., Kocharński Ł., Wyszomirski M. A case study on building information (BIM) and land information (LIM) models including geospatial data. *Geomat. Env. Eng.* 2023, 17(1) <https://doi.org/10.7494/geom.2023.17.1.19>
 53. Borkowski A.S., Łuczkiwicz N. Landscape information model (LIM): a case study of Ołtarzew Park in Ożarów Mazowiecki municipality. *Bud. Architekt.* 2023, 22(2), 41–56. <https://doi.org/10.35784/bud-arch.3547>
 54. Kurczyński Z., Bakula K., Karabin M., Kowalczyk M., Markiewicz J.S., Ostrowski W., Podlasiak P., Zawieska D. The possibility of using images obtained from the UAS in cadastral works. *Int. Arch. Photogramm. Remote Sens. Spatial Inf. Sci.* 2016, XLI-B1, 909–915. <https://doi.org/10.5194/isprs-archives-XLI-B1-909-2016>
 55. Karabin M., Bakula K., Łuczyński R. Verification of the geometrical representation of buildings in cadastre using UAV photogrammetry. *Geomat. and Environ. Eng.* 2021, 15, 4. <https://doi.org/10.7494/geom.2021.15.4.81>
 56. Puniach E., Bieda A., Cwiąkała P., Kwartnik-Pruc A., Parzych P. Use of unmanned aerial vehicles (UAVs) for updating farmland cadastral data in areas subject to landslides. *ISPRS Int. J. Geo-Inf.* 2018, 7, 331. <https://doi.org/10.3390/ijgi7080331>
 57. Crommelinck S., Bennett R., Gerke M., Yang M.Y., Vosselman G. Contour detection for UAV-based cadastral mapping. *Remote Sens.* 2017, 9, 171. <https://doi.org/10.3390/rs9020171>
 58. Crommelinck S., Höfle B., Koeva M.N., Yang M.Y., Vosselman G. Interactive cadastral boundary delineation from UAV data. *ISPRS Ann. Photogramm. Remote Sens. Spatial Inf. Sci.* 2018, IV-2, 81–88. <https://doi.org/10.5194/isprs-annals-IV-2-81-2018>
 59. Šafář V., Potůčková M., Karas J., Tlustý J., Štefanová E., Jančovič M., Cígler Žofková D. The Use of UAV in Cadastral Mapping of the Czech Republic. *ISPRS Int. J. Geo-Inf.* 2021, 10, 380. <https://doi.org/10.3390/ijgi10060380>
 60. Pyka K. Wiącek P. Guzik M. Surveying with photogrammetric unmanned aerial vehicles. *Arch. of Photogramm. Cartogr. and Remote Sens.* 2020, 32, 79–102. <https://doi.org/10.14681/apcrs.2020.0004>
 61. Directive 2007/2/EC of the European Parliament and

- of the Council of 14 March 2007 establishing an Infrastructure for Spatial Information in the European Community (INSPIRE). OJEU L 108/1 of 25.04.2007.
62. Act of 4 March 2010 on spatial information infrastructure. Journal of Laws 2010 No. 76 Item 489 as Amended. <https://isap.sejm.gov.pl/isap.nsf/download.xsp/WDU20100760489/U/D20100489Lj.pdf> (Accessed: 04.06.2024).
63. Regulation of the Minister of Development, Labor and Technology of 23 July 2021 on the database of topographic objects and the basic map. Journal of Laws 2021 Item 1385. <https://isap.sejm.gov.pl/isap.nsf/download.xsp/WDU20210001385/O/D20211385.pdf> (Accessed: 04.06.2024).
64. Regulation of the Minister of Development of 18 August 2020 on technical standards for the performance of geodetic situational and height measurements as well as the development and transfer of the results of these measurements to the state geodetic and cartographic resource. Journal of Laws 2020 Item 1429. <https://isap.sejm.gov.pl/isap.nsf/download.xsp/WDU20200001429/O/D20201429.pdf> (Accessed: 04.06.2024).
65. Ferrer-González E., Agüera-Vega F., Carvajal-Ramírez F., Martínez-Carricondo P. UAV photogrammetry accuracy assessment for corridor mapping based on the number and distribution of ground control points. *Remote Sens.* 2020, 12, 2447. <https://doi.org/10.3390/rs12152447>
66. He G.B., Li L.L. Research and application of LIDAR technology in cadastral surveying and mapping. *Int. Arch. Photogramm. Remote Sens. Spat. Inf. Sci.* 2020, 43, 33–37. <https://doi.org/10.5194/isprs-archives-XLIII-B1-2020-33-2020>